Analytica Chimica Acta 701 (2011) 66–74

Contents lists available at ScienceDirect

Analytica Chimica Acta

journal homepage: www.elsevier.com/locate/aca

An amperometric biosensor based on acetylcholinesterase immobilized onto iron oxide nanoparticles/multi-walled carbon nanotubes modified gold electrode for measurement of organophosphorus insecticides

Nidhi Chauhan, Chandra Shekhar Pundir*

Department of Biochemistry, M.D. University, Rohtak 124001, Haryana, India

HIGHLIGHTS

- Constructed a novel composite material using Fe_3O_4NP and c-MWCNT at Au electrode for electrocatalysis.
- The properties of nanoparticles modified electrodes were studied by SEM, FTIR, CVs and EIS.
- The biosensor exhibited good sensitivity (0.475 mA μM^{-1})
- The half life of electrode was 2 months.
- The sensor was suitable for trace detection of OP pesticide residues in milk and water.

GRAPHICAL ABSTRACT

The stepwise amperometric biosensor fabrication process and immobilized acetylcholinesterase inhibition in pesticide solution.

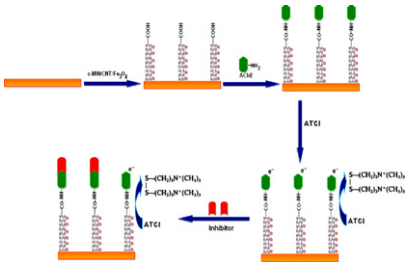

ARTICLE INFO

Article history:
Received 4 February 2011
Received in revised form 5 May 2011
Accepted 9 June 2011
Available online 17 June 2011

Keywords:
Acetylcholinesterase
Iron oxide nanoparticles
Multi walled carbon nanotubes
Organophosphorus pesticides
Amperometric biosensor

ABSTRACT

An acetylcholinesterase (AChE) purified from maize seedlings was immobilized covalently onto iron oxide nanoparticles (Fe_3O_4NP) and carboxylated multi walled carbon nanotubes (c-MWCNT) modified Au electrode. An organophosphorus (OP) biosensor was fabricated using this AChE/Fe_3O_4/c-MWCNT/Au electrode as a working electrode, Ag/AgCl as standard and Pt wire as an auxiliary electrode connected through a potentiostat. The biosensor was based on inhibition of AChE by OP compounds/insecticides. The properties of nanoparticles modified electrodes were studied by scanning electron microscopy (SEM), Fourier transform infrared (FTIR), cyclic voltammograms (CVs) and electrochemical impedance spectroscopy (EIS). The synergistic action of Fe_3O_4NP and c-MWCNT showed excellent electrocatalytic activity at low potential (+0.4 V). The optimum working conditions for the sensor were pH 7.5, 35 °C, 600 μM substrate concentration and 10 min for inhibition by pesticide. Under optimum conditions, the inhibition rates of OP pesticides were proportional to their concentrations in the range of 0.1–40 nM, 0.1–50 nM, 1–50 nM and 10–100 nM for malathion, chlorpyrifos, monocrotophos and endosulfan respectively. The detection limits were 0.1 nM for malathion and chlorpyrifos, 1 nM for monocrotophos and 10 nM for endosulfan. The biosensor exhibited good sensitivity (0.475 mA μM^{-1}), reusability (more than 50 times) and stability (2 months). The sensor was suitable for trace detection of OP pesticide residues in milk and water.

1. Introduction

Organophosphorus (OP) insecticides are widely used in agriculture. Their presence in water, food and animal feeds presents a potential hazard due to their high mammalian toxicity [1]. The most general approach for determination of the organophosphorus compounds is based on their property of inhibiting some important enzymes [2], e.g. acetylcholinesterase (AChE), which is essential for the functioning of the central nervous system but whose inactivity causes respiratory paralysis and death [3]. Hence, a rapid and reliable quantification of trace level of OP compounds is important for monitoring their potential hazard to health and the environment

* Corresponding author. Tel.: +91 9416492413; fax: +91 126274640.
E-mail address: pundircs@rediffmail.com (C.S. Pundir).

0003-2670/$ – see front matter © 2011 Elsevier B.V. All rights reserved.
doi:10.1016/j.aca.2011.06.014

[4]. In view of the unavoidable routes of OPs into biological systems, different analytical methods and technologies have been used to determine them. Presently, the most common techniques are gas chromatography [5], high-performance liquid chromatography [6] and gas chromatography coupled with mass spectrometry [7]. Although these methods provide very good sensitivity and accuracy, these are currently limited to laboratory analysis, due to the requirements of sophisticated and expensive equipment, extensive time, highly trained personnel and complicated sample pretreatments [8]. Hence, rapid, sensitive and field deployable methods are still needed for simple, rapid and reliable detection of OP.

As a good alternative and with the improvement of being quick and consistent, biosensors based on inhibition of enzyme acetylcholinesterase and coupled with simple detectors were developed recently [9–16], which are considered a viable alternative to the chromatographic methods in pesticide determination for on-site analysis. Besides being specific and sensitive, they are portable, less expensive and do not require tedious sample pretreatment [17]. Various nanoparticles based enzyme (AChE) electrodes have been reported for determination of pesticides such as ZrO_2 NPs-modified screen printed electrode [18], multi-walled carbon nanotube modified GCE [19], AuNPs–polypyrrole nanowires composite film modified GCE [20], gold–platinum bimetallic nanoparticles onto 3-aminopropyltriethoxy silane modified GC electrode [21], Au-MWNTs-modified GC electrode [22], one-dimensional gold nanoparticles onto GC electrode [23] and prussian blue modified GC electrode [24]. However these electrodes suffer from leakage of enzyme resulting into low stability of enzyme electrode and require several operations involving pretreatment of the sample. In electrochemical studies, electrodes made up of commonly used solid materials, such as graphite, carbon paste and glassy carbon (GC), exhibit common disadvantages, e.g. the electrode area and the activity of the metal deposited electrically change continuously and oxide layers affecting the reproducibility of the measurements [25]. Covalent immobilization of enzyme not only overcomes this problem but also leads to better biomolecule activity and greater stability.

Carbon nanotubes (CNT) are the promising nanomaterials recently explored for chemical and biological sensing application. They are hollow graphitic cylinders with electrocatalytic effect and a fast electron-transfer rate [26–28]. Among a wide variety of metal oxide nanoparticles, Fe_3O_4 nanoparticles are particularly attractive due to their unique magnetic and electrical properties [29]. Nano-sized magnetic bioconjugated materials have been used in electrochemical biosensor devices due to many potentially unique properties such as large surface area, higher bioactivity, excellent conformation stability and better contact between biocatalyst and its substrate [30,31]. We describe herein a unique approach of immobilizing covalently maize acetylcholinesterase onto Fe_3O_4/c-MWCNT modified gold electrode (AuE) and its application in construction of an amperometric biosensor for determination of pesticides. Fe_3O_4/c-MWCNT nanocomposite based AChE biosensor is expected to offer high sensitivity, high biocompatibility, high charge transfer rate and good stability.

2. Experimental

2.1. Chemical and reagents

Acetylthiocholine chloride (ATCl), 2-pyridine aldoxime methiodide [2-PAM], Sephadex G-100 and DEAE-Sephacel from Sigma Chemical Co., USA. 5,5′-dithiobis(2-nitrobenzoic acid) (DTNB), $(NH_4)_2{\cdot}Fe(SO_4)_2{\cdot}6H_2O$ and $NH_4Fe(SO_4)_2{\cdot}6H_2O$ from Sisco Research Laboratory, Mumbai, carboxylated multi-walled carbon nanotubes (Functionalized MWCNT or c-MWCNT) (12 walls, length 15–30 μm, Purity 90%, Metal content: nil) from Intelligent Materials Pvt. Ltd., Panchkula (Haryana) India were used. The pesticides (malathion, chlorpyrifos, monocrotophos and endosulfan) were from Lentrek North America (San Francisco, CA). Au wire (1.5 cm × 0.05 cm) (23 carat) was from local market. All other chemicals were of analytical reagent (AR) grade. Double distilled water was used throughout the experiments.

2.2. Apparatus

Cyclic voltammetry (CV), differential pulse voltammetry (DPV) and electrochemical impedance spectroscopy (EIS) measurements were performed on a potentiostat/Galvanostat (Autolab, Eco Chemie, The Netherland. Model: AUT83785) with a three electrode system composed of a platinum wire as an auxiliary electrode, an Ag/AgCl electrode as reference electrode and modified Au wire as a working electrode. Fourier transform infrared (FTIR) spectroscopy was performed in spectrometer (model iS10, Thermoelectron, USA). Ultrasonication was performed on Misonix Ultrasonic Liquid Processors (mode XL-2000 series). Scanning electron microscopy (SEM) measurements were carried out at Department of Chemistry, M.D. University, Rohtak. X-ray diffraction (XRD) studies of Fe_3O_4NP and c-MWCNT were carried out at Physics Department G. J. University, Hisar, using X-ray diffractometer (make: Rigaku Mini Flex II, Americas Corporation).

2.3. Purification of AChE from maize seedlings

The extraction and purification of enzyme was carried out in cold (4–10 °C). Two hundred grams of 5-day-old etiolated maize seedlings were homogenized in a 4-fold volume (w/v) of 10 mM potassium phosphate buffer (pH 7.0) containing 10 mM EDTA and 4% ammonium sulfate. The homogenate was left for 1 h in the dark, and then the supernatant was collected by centrifugation at 6000 × *g* for 15 min and stored at 4 °C. The pellet was resuspended in a 3-fold volume (w/v) of the extraction buffer, stirred for 1 h and recentrifuged for collection of supernatant. This procedure was repeated twice. The supernatants were combined and brought to 80% saturation with ammonium sulfate and left overnight. The resulting precipitates were collected by centrifugation at 15,000 × *g* at 4 °C for 15 min, resuspended in 3 mL of 10 mM phosphate-buffered saline, pH 7.4 and then dialyzed against the same buffer. The precipitate that formed during dialysis was removed by centrifugation and the supernatant was subjected to gel filtration on Sephadex G-100 column (1.4 cm × 23 cm) run in 0.05 M potassium phosphate buffer (pH 7.0) and ion exchange chromatography on DEAE-Sephacel column (2.5 cm × 12.5 cm) using a linear gradient of 0.1 M to 0.6 KCl in 0.02 M potassium phosphate buffer (pH 6.7) [32]. The active fractions were pooled and treated as purified enzyme.

2.3.1. Testing of purity of AChE

The purity of purified enzyme was tested by polyacrylamide gel electrophoresis (PAGE) using Coomassie blue as protein stain.

2.3.2. AChE assay

AChE preparation (100 μL) was added to 150 μL of distilled water. After pre-incubation at 30 °C for 10 min, 250 μL of 12.5 mM acetylthiocholine chloride in 100 mM sodium phosphate buffer, pH 7.0, was added to diluted enzyme and incubated again at same temperature (30 °C) for 120 min. After incubation, 300 μL of the reaction mixture was transferred to a new vial, and then 1425 μL of 100 mM sodium phosphate buffer, pH 7.0 and 75 μL of DTNB in 100 mM sodium phosphate, pH 7.0, were added to this vial. The A_{412} was read after 1 min. The control was run in the same manner as described above except that the enzyme was replaced by D.W [32].

One enzyme unit is defined as 1 μmol of thiol group appearance min^{-1} [32]. The enzyme activity was calculated using the following formula:

$$R = 5.74 \times 10^{-4} \times A/CO$$

where R = rate in moles of substrate hydrolyzed min^{-1} g^{-1} tissue, A = change in absorbance at 412 nm min^{-1}, CO = original concentration of the tissue (mg mL^{-1}).

2.4. Preparation of Fe_3O_4 nanoparticles and their deposition onto c-MWCNTs composite

Fe_3O_4NP were prepared [33] with little modification. First, 0.265 g of $(NH_4)_2{\cdot}Fe(SO_4)_2{\cdot}6H_2O$ and 0.059 g of $NH_4Fe(SO_4)_2{\cdot}6H_2O$ were dispersed into 200 mL of distilled water by strong stirring. Then 1.0 mg of c-MWCNTs was added to the solution with ultrasonic treatment for about 10 min. Finally, 0.4 mol L^{-1} sodium hydrate solution was added drop-wise into the solution until its pH reached 7.0. After stirring for 30 min and deposition at 50 °C for 2 h, a magnet was used to separate the product from the mixture. Afterwards, the black coloured precipitates were washed with the distilled water several times until pH reached 7.0. The washed Fe_3O_4/c-MWCNTs composites were treated with pure methanol and then desiccated at 50 °C for 6 h. The modification of Fe_3O_4NP and c-MWCNT was characterized by X-ray diffraction technique.

2.5. Construction of Fe_3O_4NP/c-MWCNT modified Au electrode

A polycrystalline Au electrode (1.5 cm × 0.05 cm) was first polished with alumina slurry and then cleaned ultrasonically with ethanol and double distilled water. It was then cleaned electrochemically by cycling the electrode with potential between +1.6 and −0.4 V in 0.5 mol L^{-1} H_2SO_4 until a stable voltammogram was obtained. After washing with distilled water by sonication, the Au electrode was spread with 20 μL of Fe_3O_4/c-MWCNT solution. The electrode was dried in air and then rinsed with double distilled water.

2.6. Preparation of the working enzyme electrode

The working enzyme electrode was prepared by mounting a 10 μL of AChE solution (2 mg mL^{-1}) on the Fe_3O_4/c-MWCNT/Au electrode and keeping it at 4 °C for 24 h. It was rinsed clearly. The enzyme electrode was dried and stored at 4 °C until use.

2.7. Characterization of enzyme electrode

The modification of Au electrode surface by Fe_3O_4NP and c-MWCNT was characterized by SEM technique. The fabricated electrodes (Fe_3O_4NP/c-MWCNT/AuE and AChE–Fe_3O_4/c-MWCNT/AuE) were also characterized using FTIR and electrochemical impedance spectroscopy techniques. FTIR spectroscopy was performed in spectrometer (model iS10, Thermoelectron, USA) to check the binding of AChE with Fe_3O_4NP/c-MWCNT composite film. EIS studies were carried out in the frequency range of 0.01 Hz to 10 kHz, amplitude +0.4 V, were conducted on an Autolab Potentiostat/Galvanostat (Eco Chemie, Netherlands).

2.8. Electrochemical measurement

Electrochemical measurements were performed with potentiostat with a conventional three-electrode system comprising Pt wire as auxiliary electrode, Ag/AgCl electrode as reference and AChE immobilized on nanocomposites modified Au electrode (AChE–Fe_3O_4NP/c-MWCNT/AuE) as working electrode. Electrode was pre-equilibrated at +0.4 V for 15 s before each run of detection and the steady current readings were obtained at +0.4 V. The AChE–Fe_3O_4NP/c-MWCNT/AuE biosensor was tested amperometrically at a potential of +0.4 V. ATCl (100 μL of 0.5 mM solution) was injected into the cell containing 10 mL phosphate buffer (0.1 M, pH 7.0). The substrate (ATCl) was enzymatically hydrolyzed to thiocholine, which was then subjected to electrocatalytic oxidative dimerisation at +0.4 V vs. Ag/AgCl reference electrode to give the disulphide compound. This response, due to the oxidation of the thiocholine at the working electrode, was correlated to the activity of AChE.

$$\text{ATCl} + H_2O \xrightarrow{AChE} \text{Thiocholine} + CH_3COOH$$

$$2\ \text{Thiocholine} \xrightarrow[+0.4\ V]{\text{anodic oxidation}} \text{S—(CH}_2\text{)}_2\text{N}^+\text{(CH}_3\text{)}_3 \text{ (S—(CH}_2\text{)}_2\text{N}^+\text{(CH}_3\text{)}_3\text{)} + 2H^+ + 2e^-$$

Optimization of acetylcholine measurements with AChE–Fe_3O_4NP/c-MWCNT/Au electrode was accomplished by testing at different pH 5.5–10.0 buffers using: phosphate buffer (pH 5.5, 6.0, 6.5, 7.0 and 7.5) and borate buffer (pH 8.0, 8.5, 9.0 and 10.0) each at 0.1 M final concentration containing 0.1 M potassium chloride. To determine optimum temperature, the reaction mixture was incubated at 20–55 °C at an interval of 5 °C. To study the effect of substrate concentration, different ATCl concentrations, ranging from 0.1 to 600 μM were tested by cyclic voltammetry from 0.0 and +1.5 V at a rate of 20 mV s^{-1}. The amperometric response was also measured in presence of potential interfering metals ions (Zn(II), Cu(II), Cd(II), Ni(II), Fe(III), Pb(II), Hg(II), Cr(VI) and Cr(III)) each at 2 μM concentration. The signal for a fixed concentration of acetylcholine was finally compared with the signal obtained in the presence of the two interfering species viz. ascorbic acid and uric acid both at 0.1 mM each.

2.9. Analytical application

2.9.1. Inhibition by pesticides

For measurements of pesticides, the AChE–Fe_3O_4NP/c-MWCNT/Au electrode was first immersed into 0.1 M phosphate buffer solution (pH 7.5) containing different concentrations of standard malathion (0.1–40 nM) or other pesticides for 12 min, and then transferred to the electrochemical cell consisting of 10.0 mL, 0.1 M phosphate buffer (pH 7.5) containing 0.5 mM ATCl to study the electrochemical response by cyclic voltammetry. The inhibition of malathion was calculated as follows:

$$\text{Inhibition}\,(\%) = 100 \times \frac{i_{p,\text{control}} - i_{p,\text{exp}}}{i_{p,\text{control}}}$$

where $i_{p,\text{control}}$ is the peak current of ATCl on AChE–Fe_3O_4NP/c-MWCNT/AuE, $i_{p,\text{exp}}$ is the peak current of ATCl on AChE–Fe_3O_4NP/c-MWCNT/AuE with malathion inhibition.

2.9.2. Enzyme reactivation

After exposure of AChE–Fe_3O_4NP/c-MWCNT/AuE to pesticides, it was washed with 0.1 M phosphate buffer (pH 7.5) and reactivated with 4.0 mM 2-pyridine aldoxime methiodide [2-PAM] for 10 min, then transferred to electrochemical cell of 10 mL buffer pH 7.5 containing 0.5 mM ATCl to study the electrochemical response. The reactivation efficiency (R%) was estimated as follows:

$$R\,(\%) = 100 \times \frac{i_r - i_{p,\text{exp}}}{i_{p,\text{control}} - i_{p,\text{exp}}}$$

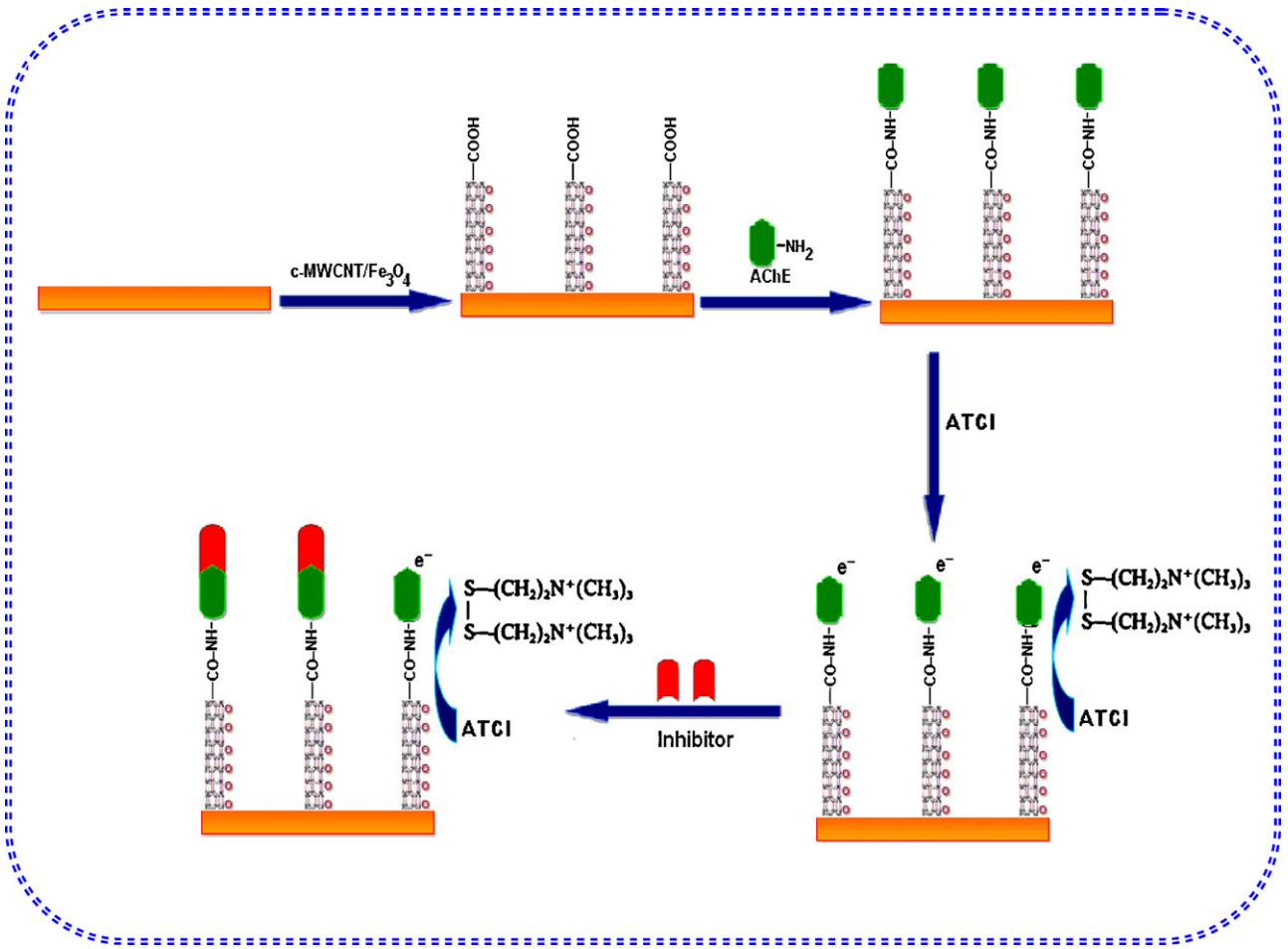

Scheme 1. Schematic illustration of the stepwise amperometric biosensor fabrication process and immobilized acetylcholinesterase inhibition in pesticide solution.

where i_r was the peak current of ATCl on AChE–Fe_3O_4NP/c-MWCNT/AuE with 2-pyridine aldoxime methiodide [2-PAM] reactivation.

2.10. Stability and reproducibility of the biosensor

To reuse the working electrode, it was washed by dipping it in phosphate buffer pH 7.5. The long-term storage and stability of the biosensor was investigated over 2-months, when AChE–Fe_3O_4NP/c-MWCNT/AuE was stored dry in a refrigerator at 4 °C. AChE–Fe_3O_4NP/c-MWCNT/AuE sensitivity was measured once in every 7 days.

3. Results and discussion

A simple and efficient chemical method was introduced for preparation of Fe_3O_4NP/c-MWCNT nanocomposite onto Au electrode. Scheme 1 illustrates that Fe_3O_4 nanoparticles were coated on the outer walls of c-MWCNTs as reported earlier [33]. Carboxyl groups present on the external surface of MWCNTs are free to bind with $–NH_2$ groups on the surface of AChE after the decoration of Fe_3O_4 nanoparticles onto the surface of c-MWCNT. The morphology of bare Au electrode, Fe_3O_4NP/c-MWCNT/Au electrode and AChE immobilized onto Fe_3O_4NP/c-MWCNT/Au electrode was characterized by SEM studies (Fig. 1). The SEM image of the bare AuE electrode (image a) showed a smooth and featureless morphology, whereas nanocomposite (image b and c) displayed a stepwise layering of Fe_3O_4NP/c-MWCNT and immobilization of AChE onto the modified Au electrode respectively.

3.1. XRD analysis of Fe_3O_4-decorated MWCNTs

As shown in Fig. 2 curve a, the (2 2 0), (3 3 1), (2 2 2), (5 1 1), (4 4 0) planes of Fe_3O_4 were observed at $2\theta = 29.82°, 35.74°, 43.06°, 57.02°, 62.78°$, respectively. It can be seen that the diffraction peaks at $2\theta = 26.08°, 43.08°$ are assigned to (0 0 2), (1 1 0) planes of MWCNTs in Fig. 2 curve b. These two diffraction peaks are attributed to the graphitic structure of MWCNTs [34]. The graphitic structure of MWCNTs was not destroyed after they were coated with Fe_3O_4 nanoparticles, as proved by the characteristic peaks of MWCNTs still existed in Fig. 2 curve a.

3.2. FT-IR analysis

In Fig. 3, the characteristic absorption peaks of c-MWCNTs were observed near 1518, 1156 and 2320 cm^{-1} respectively, which were originated from the graphitic component of c-MWCNTs. A sharp absorption peak was observed at 1640 cm^{-1} due to the attachment of carboxyl group onto the surface of MWCNTs since carboxyl groups attached to MWCNTs were merely partly replaced by Fe_3O_4 nanoparticles (curve i). In the FTIR spectrum of AChE–Fe_3O_4NP/c-MWCNT/Au electrode (curve ii), enzyme (AChE) binding is indicated by the appearance of additional absorption bands at 1641 and 1539 cm^{-1} assigned to the carbonyl stretch (amide I band) and –N–H bending (amide II band), respectively.

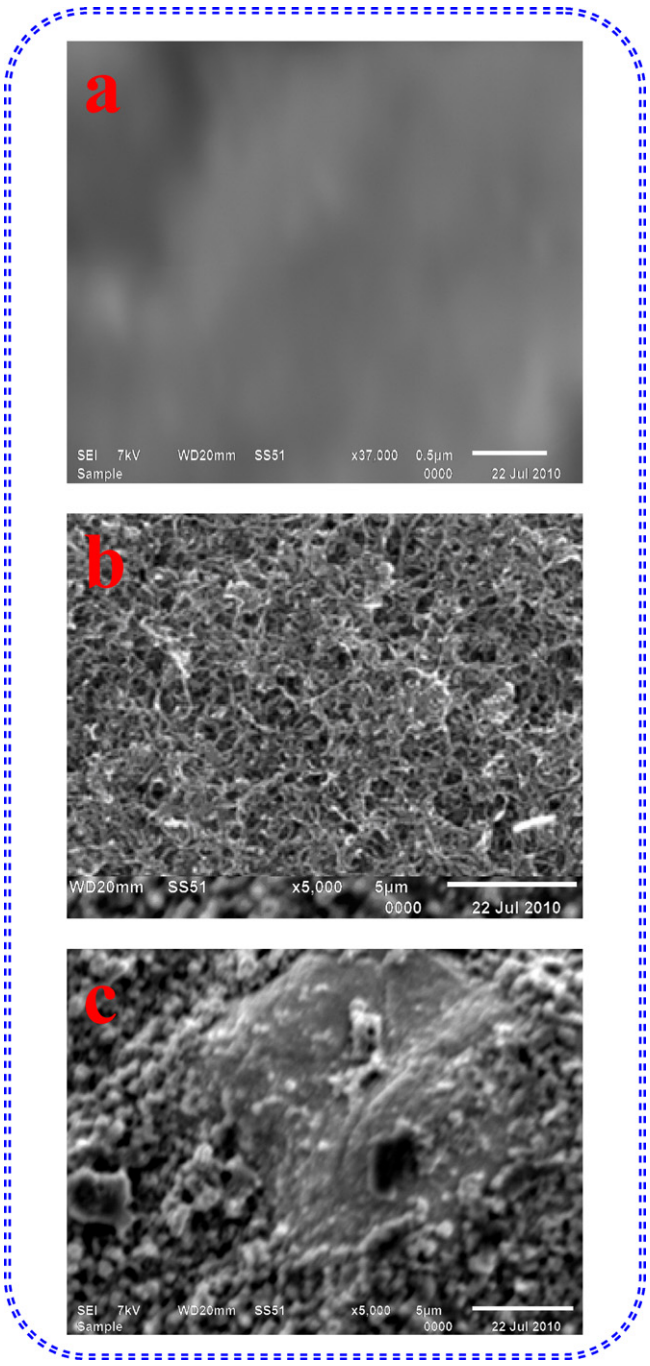

Fig. 1. Scanning electron micrographs of (a) bare Au electrode, (b) Fe_3O_4NP/c-MWCNT/Au electrode, (c) AChE/Fe_3O_4NP/c-MWCNT/Au electrode.

Also, a broad band was seen around 3200 cm^{-1}, which is attributed to amide bond present in AChE.

3.3. Electrochemical impedance spectroscopy studies

EIS is an effective method to monitor the changes of the surface modified electrodes allowing the understanding of the chemical transformation and process associated with the conductive electrode [35]. Fig. 4 exhibits the Nyquist plot of the impedance spectroscopy of the bare and modified electrodes. In EIS, the bare electrode exhibited an almost straight line (Fig. 4a), which is characteristic of a diffusional limiting step of the electrochemical process. The Nyquist plot of c-MWCNT modified Au electrode (Fig. 4b) gave

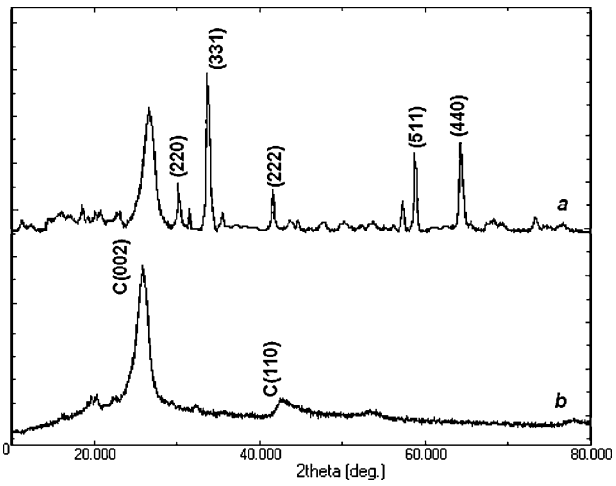

Fig. 2. XRD patterns of Fe_3O_4NP/c-MWCNTs/(a) and c-MWCNTs (b).

an Rct value of 120 Ω. c-MWCNT coated Fe_3O_4 modified Au electrode (Fig. 4c) possessed a remarkably low Rct (75 Ω), implying that the c-MWCNT coated Fe_3O_4 are acting as good electron conducting materials and there was the electron transfer between the redox probe and the electrode. When compared to the nanocomposite modified electrode, the semicircle diameter was increasing with the immobilization of AChE on Fe_3O_4NP/c-MWCNT modified Au electrode, showing an Rct value of 175 Ω (Fig. 4d), confirming the immobilization of enzyme, which reduced the electron transfer between the redox probe and the electrode. The above results confirm the success of the assembly on the electrode.

3.4. Electrochemical characterization of the AChE–Fe_3O_4NP/c-MWCNT biosensor

In the developed amperometric biosensor, AChE was covalently immobilized on Fe_3O_4NP/c-MWCNT/AuE. The performance of the working Au electrode during stepwise modification was also evaluated by CV in 0.1 M phosphate buffer (pH 7.5). Fig. 5 showed the cyclic voltammograms of AuE, Fe_3O_4NP/c-MWCNT/AuE and AChE–Fe_3O_4NP/c-MWCNT/AuE in presence of 100 μL of ATCl (0.6 mM) in phosphate buffer (pH 7.5) at a scan rate of 20 mV s^{-1}. No peak was observed for AuE (curve a) in phosphate buffer after 100 μL of ATCl was injected into reaction cell. The cyclic voltammogram of Fe_3O_4NP/c-MWCNT/AuE identified an oxidation peak at +125 mV (curve b), and the modified AChE–Fe_3O_4NP/c-MWCNT/AuE also showed an oxidation peak at +375 mV (curve c). The oxidation peak (curve c) came from the oxidation of thiocholine, hydrolysis product of ATCl, catalyzed by immobilized AChE. Fig. 5 also showed that this peak current (curve c) had a sharp increase and the peak potential shifted negatively compared to those on the electrode without AChE (curve c). Main reason was the presence of Fe_3O_4NP on the surface of AuE, which possessed a relatively large specific surface area and an inherent, high electricity conducting ability. Thus they could enhance the rates of catalyzed reactions as well as the electron transfer rate at a lower potential [36].

3.5. Optimization of experimental parameters

The pH dependence of the biosensor response in 0.1 M phosphate buffer (pH 5.5, 6.0, 6.5, 7.0 and 7.5) and borate buffer (pH 8.0, 8.5, 9.0 and 10.0) in 5.0–8.0 range was studied. The response current changed slightly between pH 5.0 and pH 7.0 but the maximum current was observed at pH 7.5. However, the enzyme lost activity

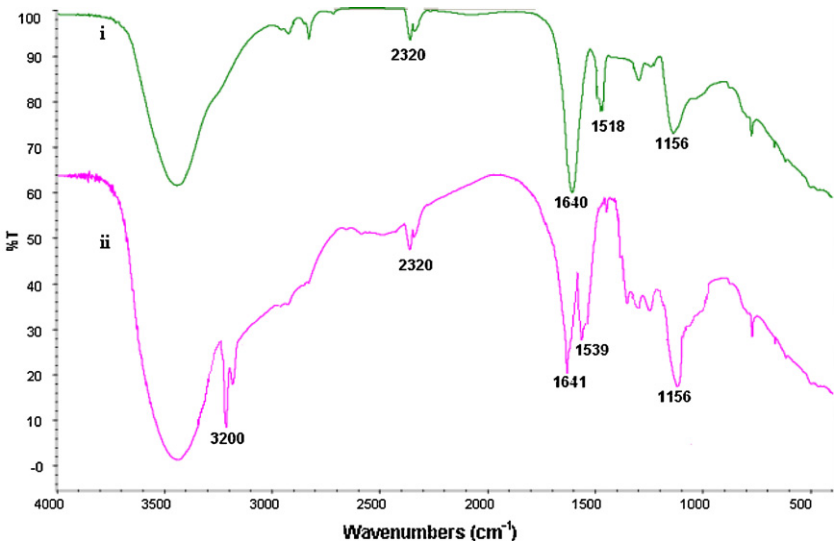

Fig. 3. The infrared spectra of Fe_3O_4NP/MWCNT/AuE without enzyme (i) and with enzyme (ii).

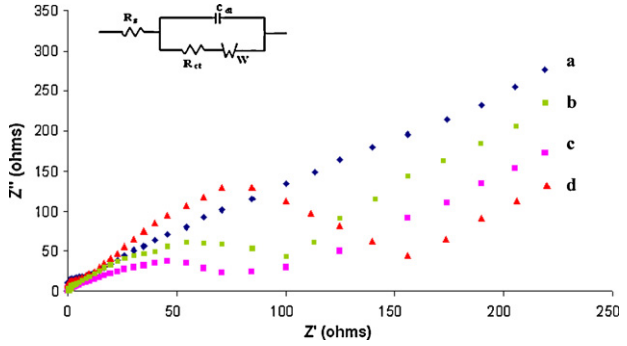

Fig. 4. Electrochemical impedance Nyquist plot of bare AuE (a), c-MWCNT/AuE (b), Fe_3O_4NP/c-MWCNT/AuE (c) and AChE–Fe_3O_4NP/c-MWCNT/AuE (d) at 0.1 M phosphate buffer (pH 7.5) containing 0.5 mM $[Fe(CN)_6]^{3-}$ + 0.5 mM $[Fe(CN)_6]^{4-}$ and 0.5 mM acetylthiocholine. Frequency range: 0.01 Hz to 10 kHz. Inset shows the equivalent circuit for 'mixed kinetic and diffusion control'.

irreversibly at the lower or higher pH values. Therefore, phosphate buffer of pH 7.5 was selected for subsequent experiments. The effect of the temperature on the biosensor response from 20 to 50 °C was also investigated. No significant change in current response was observed during this temperature range, but slightly peaked at 35 °C. Hence, the optimum temperature (35 °C) was selected for subsequent experiments. The microenvironment provided by nanocomposite around the enzyme has increased its thermal stability, similar to earlier report of increased thermal stability of this enzyme by a microenvironment of assembling of MWCNT and silica

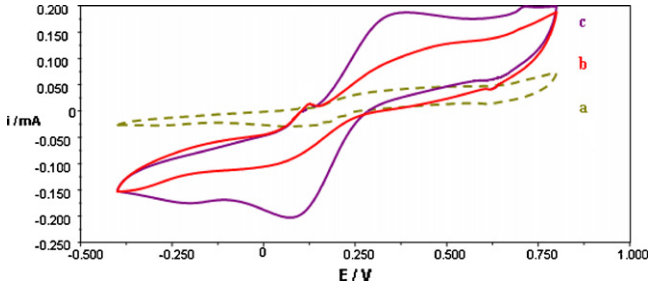

Fig. 5. Cyclic voltammograms, AuE (a); Fe_3O_4NP/c-MWCNT/AuE (b) and AChE–Fe_3O_4NP/c-MWCNT/AuE (c) in pH 7.5 sodium phosphate containing (0.1 M) 100 μL of ATCl (0.5 mM). Scan rate: 20 mV s^{-1}.

sol gel [37]. The increased thermal stability of immobilized enzyme could be due to the biocompatible microenvironment around the enzyme molecule provided by the Fe_3O_4NP/c-MWCNT, which stabilizes their biological activity to a large extent. The concentration of ATCl was optimized by studying cyclic voltammetry study as well as chronoamperometry of AChE–Fe_3O_4/c-MWCNT/AuE in the cell solution containing ATCl substrate under optimum conditions. Fig. 6A and B show well defined increasing trend in the current response of the biosensor from 0.1 to 600 μM ATCl concentrations. In the absence of ATCl, the peak responses were negligible. Fig. 6 B shows a typical current–time plot was plotted against concentrations of ATCl. Voltammetric measurements were performed after each addition of the ATCl up to a maximum concentration of 600 μM. There was no significant current improvement after 600 μM of ATCl concentration. The electrode had reached its saturation level at 700 μM. The time required to attain the 95% of the steady state response was within 4 s, which indicated a very fast diffusion process. A good linear relationship of response current with substrate concentration from 0.1 to 600 μM is evident from both the studies. Over a concentration range of 0.1–600 μM, the electrode provided a linear response to ATCl with a sensitivity of 0.475 mA μM^{-1} better than earlier reports [38,39]. From these results, 600 μM of ATCl was selected as optimum concentration for further experiments.

3.6. Incubation time on inhibition

Pesticides detection studies were carried out at saturating substrate concentration (0.6 mM). Each pesticide at final concentration of 1.0 nM was tested in terms of their effect on enzyme activity at different incubation times in pesticide solution (2–20 min at an interval of 2 min). It can be seen that inhibition of the enzyme was increased (up to 80%) with increasing incubation time, i.e. up to 10 min after which it was almost constant for each pesticide (Fig. 7). Therefore the incubation time was selected as 10 min for each pesticide. Fig. 7 displays increased inhibition on AChE with increased inhibition time. When the inhibition time is longer than 10 min, the curve tends to a stable value, indicating the binding interaction between pesticides and active target groups in the enzyme reaches saturation. However, the maximum value of inhibition of pesticides was not 100%, which is attributable to the binding equilibrium between pesticides and binding sites in the enzyme. This value compares favorably with most of the data reported in the

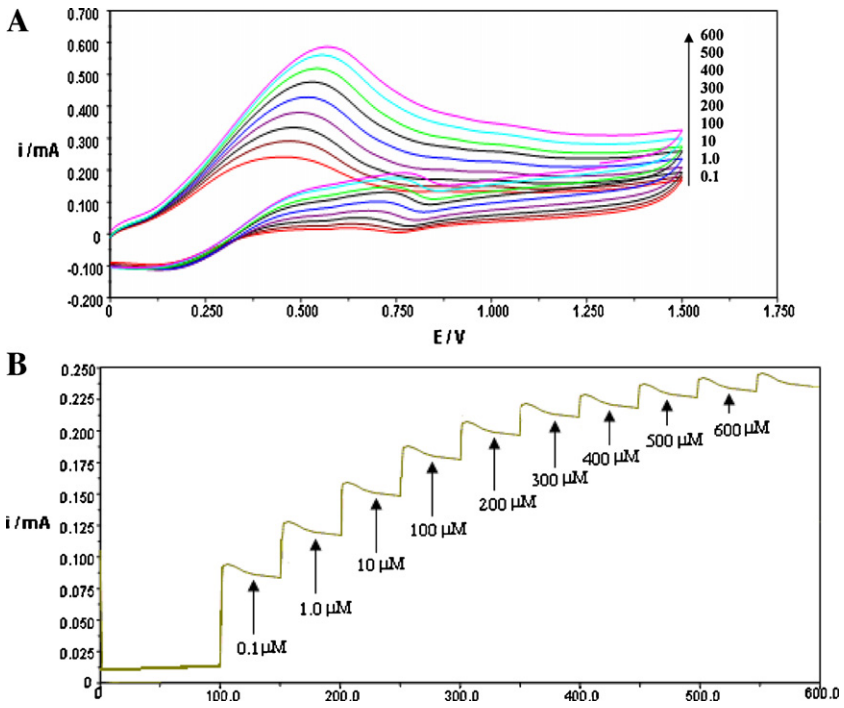

Fig. 6. (A) Effect of substrate concentration on response of AChE–Fe_3O_4NP/c-MWCNT modified Au electrode in 0.1 M sodium phosphate buffer solution (pH 7.5) at a potential range of 0 to +1.5 V, scan rate 20 mV s^{-1} vs. Ag/AgCl reference electrode. (B) Current–time responses curve of the AChE–Fe_3O_4NP/c-MWCNT modified Au electrode with successive addition of ATCl into 0.1 M sodium phosphate buffer solution (pH 7.5). Applied potential + 0.4 V vs. Ag/AgCl reference electrode.

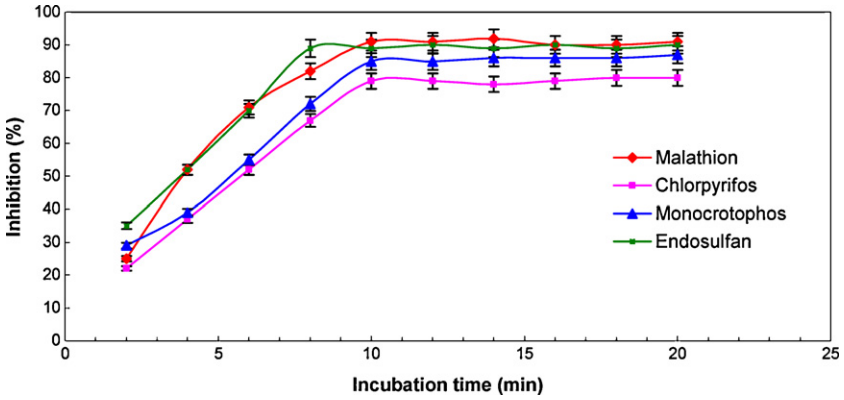

Fig. 7. The effect of incubation time on inhibition. Response of the pesticide biosensor to 0.06 M acetylthiocholine chloride and 1.0 nM pesticide. Buffer: 0.1 M sodium phosphate buffer, pH 7.5, with 0.1 M KCl. Applied potential + 0.4 V vs. Ag/AgCl.

literature [39–41]. Yang et al. [39], Viswanathan et al. [40] and Ghosh et al. [41] used an incubation time of 15 min respectively, for chlorpyrifos, malathion and monocrotophos detection.

3.7. Response characteristics of the biosensor

3.7.1. Linear working range and detection limit

The detection limit and the linear working range of the biosensor were evaluated for different pesticides. Incubation method (10 min incubation time) was used in the detection measurement. At 20–30% enzyme inhibition level, the detection limit for malathion, chlorpyrifos, monocrotophos and endosulfan was found to be 0.1–40 nM, 0.1–50 nM, 1–50 nM and 10–100 nM respectively. Measurement of the pesticides concentration at site lower levels of enzyme inhibition was avoided because some interferent can also inhibit the enzyme to a small extent. Therefore, 20–30% enzyme inhibition level was considered as optimum. The linear range for malathion, chlorpyrifos, monocrotophos and endosulfan was achieved as 0.1 nM, 0.1 nM, 1.0 M and 10 nM respectively, which is lower than earlier reported biosensors (10 nM for malathion [39], 50 nM for paraoxon ethy [21], 1 nM for paraoxon [22] and 7 nM for methamidophos [23]). Earlier it was reported that acceptable levels for drinking of malathion and chlorophrifos in tap water was 0.99 and 0.1 µg L^{-1} (2.9 and 0.2 nM respectively) [42]. Hence, the developed detection system (biosensor) was highly sensitive and could detect the OPs compound in the range of nM. It showed that the biosensor has good analytical characteristics for these inhibitors due to good electrochemical catalytic efficacy of Fe_3O_4NP/c-MWCNT.

3.7.2. Precision and accuracy

The precision and accuracy of the present method were determined over 14 days. Each day 5 replicate of quality control samples were analyzed for acetylcholine content. The accuracy of the method was determined by comparing the calculated concentrations with their nominal values. The repeatability and inter-day

Table 1
Precision and accuracy of the AChE/Fe_3O_4NP/MWCNT/AuE.

Added concentration (nM)	Mean ± SD measured concentration (nM)	Repeatibility (RSD%)	Inter-day precision (RSD%)	Accuracy (%)
0.20	0.22 ± 0.03	13.63	2.00	110.0
0.80	0.85 ± 0.05	5.88	6.00	106.0
1.50	1.48 ± 0.02	1.35	1.45	98.6
3.50	3.48 ± 0.02	0. 57	1.00	99.4
8.00	8.20 ± 0.10	1.21	1.49	102.0
12.00	12.05 ± 0.50	4.14	4.00	100.4
15.00	15.02 ± 0.08	0.53	1.80	100.1

Table 2
Recoveries of malathion, chlorpyrifos, monocrotophos and endosulfan in tap water samples by AChE/Fe_3O_4NP/MWCNT/AuE.

Pesticides	Added concentration (nM)	Concentration found (nM)	% Recovery	SD (n = 3)
Malathion	0.5	0.52	104.00	3.1
	1.0	1.10	110.00	1.9
	1.5	1.46	97.33	1.8
Chlorpyrifos	1	0.95	95.00	1.4
	5	5.1	102.00	1.21
	10	10.5	105.00	2.32
Monocrotophos	0.2	0.23	115.00	1.5
	0.6	0.64	106.00	1.36
	1.0	1.1	110.00	0.57
Endosulfan	5	5.2	104.00	2.3
	10	10.9	109.00	1.6
	15	15.6	104.00	0.97

precision were less than 14% and the accuracy within 98–110%. This demonstrates that the present method was precise and accurate for determination of pesticides within the range 0.2–15.0 nM. The results are summarized in Table 1. The analytic recovery of known amount of malathion, chlorpyrifos, monocrotophos and endosulfan in tap water samples/spiked samples under optimum conditions was determined by the present biosensor. The mean analytic recoveries were in the range of 95–115% (Table 2).

3.7.3. Interference study

Theoretically speaking, heavy metal ions can inhibit the activity of AChE and disturb OPs detection using the AChE based biosensor. However, there is no actual report so far on the kind and concentration limit of heavy metal ions which can disturb OPs detection. In this study we tried to obtain actual relative information, by examining the effects of heavy metal ions, i.e. Zn(II), Cu(II), Cd(II), Ni(II), Fe(III), Pb(II), Hg(II), Cr(VI) and Cr(III)) on malathion detection by the present biosensor. Among these only, Hg(II) and Cr(VI) showed 40% and 15% effect on inhibition respectively, which is comparable to earlier report [43]. The signal for a fixed concentration of ATCl was compared with the signal obtained in the presence of the interfering species also. No noticeable changes in current were detected in the presence of ascorbic acid (0.1 mM) and uric acid (0.1 mM) respectively at the present operating potential in this system.

3.8. Pesticides determination

At saturating substrate (ATCl) concentration (0.5 mM), the decreases in biosensor differential pulse voltammetry responses after contact with pesticide solution is related only to the enzyme–inhibitor interaction (non-competitive) and does not depend on the mass transfer of both the substrate and the inhibitor from the bulk solution to the enzymatic layer. The DPV responses were associated with inhibition of the enzyme activity by the amount of pesticide added (Fig. 8). The decrease in the current can be explained as due to the result of the blocking of serine hydroxyl group by covalently bound phosphate group, which invariably reduces the overall charge of the catalytic active site [44]. The usage of the high substrate concentration (>0.5 mM) would not yield good results when the detection is carried out by simultaneous addition of analyte (malathion) and the substrate (ATCl). Under such conditions, the inhibition mechanism is competitive, so that the substrate would compete with the analyte for the enzyme active site and inhibition, especially at low analyte concentrations, could not be detected. Fig. 8 inset shows the standard curve of pesticide concentration (nM) vs. current (mA). The current response was decreased with increase in pesticide concentration.

3.9. Regeneration of acetylcholinesterase

Organophosphorus insecticides include a “nonreversible” inhibition due to a covalent link of organophosphorus based pesticides to AChE [45,46]. However, it is possible to reactivate the immobilized enzyme using 2-pyridine aldoxime methiodide (2-PAM). The reactivation usually fully regenerates the original activity after a 15 min incubation of immobilized AChE in a buffered solution

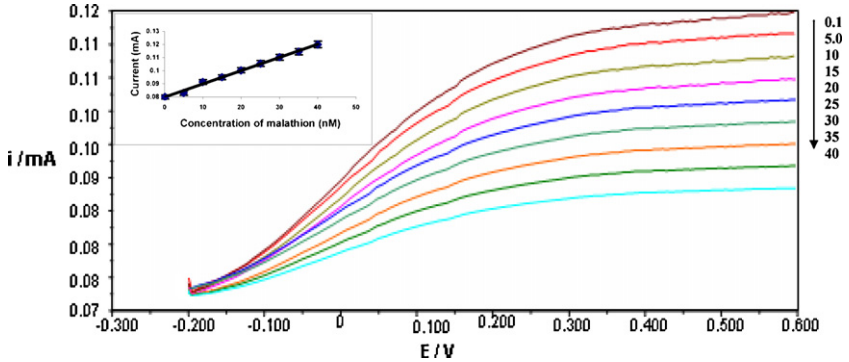

Fig. 8. DPV net current responses of biosensor after 10 min incubation with different concentrations of malathion in 0.1 M sodium phosphate buffer solution (pH 7.5) containing 0.5 mM ATCl. Scan rate: 20 mV s^{-1}. Inset: Standard curve of pesticide concentration (nM) vs. current (mA).

Table 3
Electrochemical sensing of phosphorylated AChE in milk samples by AChE/Fe_3O_4NP/MWCNT/AuE.

Milk sample	Concentration of the spiked malathion	Response current (mA)	Phosphorylated AChE (nM)	Recovery (%)
Sterilized non-fat dry milk	20	0.25	21.5 ± 2.5	107
Sterilized whole milk	40	0.45	42.6 ± 3.3	106
Clarified raw milk	80	0.70	87.3 ± 1.9	109

of 2-PAM. This reactivation allowed re-use of the biosensor and confirmed that the inhibition was due to the pesticides.

3.10. Analysis of pesticides in spiked water and milk samples

To explore the use of the biosensor for monitoring pesticides in tap water and milk, samples were spiked with malathion, chlorpyrifos, monocrotophos and endosulfan to final concentrations of 0.2 and 15 nM. Water samples without the addition of phosphorylated AChE were also evaluated. Phosphorylated AChE concentrations of the spiked samples were quantified based on the peak current intensity generated from the samples and the calibration curve depicted in inset of Fig. 8. As shown in Table 2, the recoveries for these water samples obtained from the AChE–Fe_3O_4NP/c-MWCNT/AuE sensor were calculated and found to be between 95% and 109%. Table 3 shows, the recoveries for milk samples by AChE–Fe_3O_4NP/c-MWCNT/AuE sensor between 103% and 109%. A more rigorous analysis of the analytical performance of the AChE–Fe_3O_4NP/c-MWCNT/AuE sensor for use with other samples is underway; however, these preliminary results demonstrate the potential for characterizing very low levels of OP exposure using AChE–Fe_3O_4NP/c-MWCNT matrices.

3.11. Stability and reusability of biosensor

The electrode lost 25% of its initial activity after its 50 uses during the span of 2 months, when stored at 4 °C, which is much better than earlier electrodes [39,47,48]. The good stability, repeatability and reproducibility observed for the present biosensor could be attributed to the immobilization of AChE onto Fe_3O_4NP/c-MWCNT modified Au electrode.

4. Conclusions

We constructed a novel composite of Fe_3O_4NP and c-MWCNT at Au electrode for electrocatalysis, which is stable for a long time at pH 7.5 in 0.1 M phosphate buffer solution. Furthermore the composite provides covalent immobilization of AChE on c-MWCNT as confirmed by FTIR. This AChE/Fe_3O_4NP/c-MWCNT modified Au electrode exhibited improved performance of biosensor in terms of response time (4 s), detection limit (0.1 nM), sensitivity (0.475 mA μM^{-1}), reusability (more than 50 times) and stability (2 months). Thus this work illustrates a simple and novel approach for the development of an improved amperometric enzyme sensor for pesticides determination.

Acknowledgments

Authors are grateful to Department of Science and Technology, Govt. of India, N. Delhi and Chairman, Applied Physics, Guru Jambheshwar University (GJU), Hisar for providing the instrumentation facilities for XRD studies of Fe_3O_4 and MWCNT nanoparticles.

References

[1] N. Mionettol, J.L. Marty, I. Karube, Biosens. Bioelectron. 9 (1994) 463–470.
[2] C. Cremisini, S.D. Sario, J. Mela, R. Pilloton, G. Palleschi, Anal. Chim. Acta 311 (1995) 273–280.
[3] V.B. Kandimalla, H.X. Ju, Chem. Eur. J. 12 (2005) 1074–1080.
[4] R. Solna, S. Sapelnikova, P. Skladal, M.W. Nielsen, C. Carlsson, J. Emneus, T. Ruzgas, Talanta 65 (2005) 349–357.
[5] A.D. Muccio, P. Pelosi, I. Camoni, D.A. Barbini, R. Dommarco, T. Generali, A. Ausil, J. Chromatogr. A 754 (1996) 497–506.
[6] P. Uutela, R. Reinila, P. Piepponen, R.A. Ketola, R. Kostiainen, Rapid Commun. Mass Spectrom. 19 (2005) 2950–2956.
[7] R.M. Black, R.J. Clarke, R.W. Read, M.T.J. Reid, J. Chromatogr. A 662 (1994) 301–321.
[8] G. Liu, J. Wang, R. Barry, C. Petersen, C. Timchalk, P.L. Gassman, Y. Lin, Chem. Eur. J. 14 (2008) 9951–9959.
[9] A. Andreescu, A. Avramescu, C. Bala, V. Magearu, J.L. Marty, Anal. Bioanal. Chem. 374 (2002) 39–45.
[10] H. Schulze, R.D. Schmid, T.T. Bachmann, Anal. Bioanal. Chem. 372 (2002) 268–272.
[11] F.N. Kok, F. Bozoglu, V. Hasirci, Biosens. Bioeletron. 17 (2002) 531–539.
[12] B. Bucur, D. Fournier, A. Danet, J.-L. Marty, Anal. Chim. Acta 562 (2006) 115–121.
[13] P.D. Dondoi, B. Bucur, A.F. Danet, C.N. Toader, L. Barthelmebs, J.L. Marty, Anal. Chim. Acta 578 (2006) 162–169.
[14] T.T. Bachmann, B. Leca, F. Villate, J.L. Marty, D. Fournier, R.D. Schmid, Biosens. Bioelectron. 15 (2000) 193–201.
[15] J.-L. Marty, G. Jeanty, Biosens. Bioeletron. 13 (1998) 213–218.
[16] I. Walz, W. Schwack, Eur. Food Res. Technol. 225 (2007) 593–601.
[17] I. Karube, Y. Nomura, J. Mol. Catal. B: Enzym. 10 (2000) 177–181.
[18] S. Lin, C.C. Liu, T.C. Chou, Biosens. Bioelectron. 20 (2004) 9–14.
[19] T.L. Lin, K.T. Huang, C.Y. Liu, Biosens. Bioelectron. 22 (2006) 513–518.
[20] J. Gong, L. Wang, L. Zhang, Biosens. Bioelectron. 24 (2009) 2285–2288.
[21] S. Upadhyay, G.R. Rao, M.K. Sharma, B.K. Bhattacharya, V.K. Rao, R. Vijayaraghavan, Biosens. Bioelectron. 25 (2009) 832–838.
[22] N. Jha, S. Ramaprabhu, Nanoscale 2 (2010) 806–810.
[23] L. YanRong, G. ZhiYong, L. YanFen, L. Qian, B. JianChun, D. ZhiHui, H. Min, Sci. Chin. Chem. 53 (2010) 820–825.
[24] X. Sun, X. Wang, Biosens. Bioelectron. 25 (2010) 2611–2614.
[25] Z. Jianzhong, L. Deren, Z. Guoxiong, J. Shanghai Univ. 4 (1998) 311–315.
[26] M. Zheng, A. Jagota, M.S. Strano, A.P. Santos, P. Barone, S.G. Chou, B.A. Diner, M.S. Dresselhaus, R.S. Mclean, G.B. Onoa, G.G. Samsonidze, E.D. Semke, M. Usrey, D.J. Walls, Science 302 (2003) 1545–1548.
[27] S. Viswanathan, L.C. Wu, M.R. Huang, J.A.A. Ho, Anal. Chem. 78 (2006) 1115–1121.
[28] S. Viswanathan, J. Radecki, Pol. J. Food Nutr. Sci. 58 (2008) 157–164.
[29] J.Q. Wan, W. Cai, J.T. Feng, J. Mater. Chem. 17 (2007) 1188–1192.
[30] E. Katz, I. Willner, J. Wang, Electroanalysis 16 (2004) 19–44.
[31] N. Jaffrezic-Renault, C. Martelet, Y. Chevolot, J.P. Cloarec, Sensors 7 (2007) 589–614.
[32] Y. Sagane, T. Nakagawa, K. Yamamoto, S. Michikawa, S. Oguri, Y.S. Momonoki, Plant Physiol. 138 (2005) 1359–1371.
[33] D. Cun-ku1, L. Xin, Z. Yan, Q. Jing-yao, Y. Yun-fang, Chem. Res. Chin. Univ. 25 (2009) 936–940.
[34] H.S. Chung, C.S. Chen, R.A. Kremer, J.R. Boulton, G.W. Burdette, Energy Fuels 13 (1999) 641–649.
[35] A.J. Bard, L.R. Faulkner, Electrochemical Methods: Fundamentals and Applications, third ed., Wiley, New York, 2001.
[36] L. Yang, X. Ren, F. Tang, L. Zhang, Biosens. Bioelectron. 25 (2009) 889–895.
[37] D. Du, J. Cai, D. Song, A. Zhang, J. Appl. Electrochem. 37 (2007) 893–898.
[38] S.M.A. Shibli, K.S. Beenakumari, Electroanalysis 18 (2006) 465–470.
[39] Y. Yang, M. Guo, M. Yang, Z. Wang, G. Shen, R. Yu, Int. J. Environ. Anal. Chem. 85 (2005) 163–175.
[40] S. Viswanathan, H. Radecka, J. Radecki, Biosens. Bioelectron. 24 (2009) 2772–2777.
[41] D. Ghosh, K. Dutta, D. Bhattacharyay, P. Sarkar, Environ. Monit. Assess. 119 (2006) 481–489.
[42] R. Frank, L. Logan, Arch. Environ. Contam. Toxicol. 17 (1988) 741–754.
[43] S. Sanllorente-Méndez, O. Domínguez-Renedo, M.J. Arcos-Martínez, Sensors 10 (2010) 2119–2128.
[44] K. Antoni, R. Zoran, M. Roman, R. Jessica, T. Palmer, S.K. Barry, K. Hartmuth, J. Am. Chem. Soc. 127 (2005) 6686–6692.
[45] C. Fest, K.J. Schmidt, The Chemistry of Organophosphorus Pesticides, Springer-Verlag, Berlin-Heidelberg, New York, 1973.
[46] A. Moretto, M.K. Johnson, Toxicology of organophosphates and carbamates, in: L.G. Costa (Ed.), Toxicology of Pesticides: Experimental, Clinical and Regulatory Aspects, Berlin H13, (1987) pp. 33–48.
[47] L. Doretti, D. Ferrara, S. Lora, G. Palma, Biotechnol. Appl. Biochem. 29 (1999) 67–72.
[48] S. Sanllorente-Mendez, O. Domínguez-Renedo, M.J. Arcos-Martinez, Sensors 10 (2010) 2119–2128.